Directional Tunneling and Andreev Reflection on $YBa_2Cu_3O_{7-\delta}$ Single Crystals: Predominance of d-Wave Pairing Symmetry Verified with the Generalized Blonder, Tinkham, and Klapwijk Theory

J. Y. T. Wei,[1] N.-C. Yeh,[1] D. F. Garrigus,[2] and M. Strasik[2]
[1]*Department of Physics, California Institute of Technology, Pasadena, California 91125*
[2]*Boeing Phantom Works, Seattle, Washington 98124*
(Received 29 December 1997)

We report directional tunneling and point-contact spectroscopy measurements on the {100}, {110}, and {001} faces of $YBa_2Cu_3O_{7-\delta}$ single crystals at 4.2 K. The conductance spectra show fully developed quasiparticle tunneling, Andreev reflection, and zero-bias peak characteristics, depending systematically on the junction orientation and impedance. Quantitative spectral analysis using the generalized formalism of Blonder, Tinkham, and Klapwijk (BTK) indicates a predominantly $d_{x^2-y^2}$ pairing symmetry, with less than 5% s-wave component in either the $d + s$ or $d + is$ scenario. [S0031-9007(98)07041-0]

PACS numbers: 74.50.+r, 74.72.Bk, 74.80.Fp

The issue of pairing symmetry has continued to attract interest in the field of high-temperature superconductivity (HTSC) [1]. For $YBa_2Cu_3O_{7-\delta}$ (YBCO), grain-boundary junction and corner-junction experiments sensitive to the phase of the pair-wave function in the CuO_2 plane have demonstrated $d_{x^2-y^2}$ symmetry [2–4], while Josephson tunneling measurements on Pb/Al/YBCO planar junctions perpendicular to the CuO_2 plane have indicated the presence of an s-wave order parameter [5]. Recent experiments have been reported in favor of mixed pairing symmetry in YBCO. The observation of broken time-reversal symmetry of the d-wave states for quasiparticle tunneling [6] on Cu/organic monolayer/YBCO planar junctions has been attributed to the existence of an additional out-of-phase order parameter [7], such as in the $d + is$ scenario based on surface or boundary effects [8]. The detection of an order parameter phase shift across a YBCO twin boundary by c-axis Pb/Al/YBCO Josephson tunneling [9] has provided evidence for $d + s$ pairing symmetry, as may be expected from the orthorhombic crystal structure [8].

While these results *qualitatively* address the d-wave vs s-wave controversy in YBCO, they do not provide information on the magnitudes of the component order parameters, a detailed measurement of which would help to identify the pairing interaction responsible for HTSC [1]. In principle, the highly anisotropic energy gap could be probed by tunneling spectroscopy, which is traditionally known to be sensitive to the superconducting density of states (DOS) with fine energy resolution and considerable directionality [10]. However, unlike other measurements such as angle-resolved photoemission spectroscopy (ARPES) [11], tunneling spectroscopy has shown little success in mapping out the gap anisotropy. Part of the problem could be the experimental difficulties in making highly oriented and chemically homogeneous tunnel junctions, as required by the short coherence lengths of the cuprates [12]. More importantly, theoretical studies [13–15] using the formalism of Blonder, Tinkham, and Klapwijk (BTK) [16] have indicated that the d-wave sign change about its nodal axes ($k_x = \pm k_y$) allows the formation of Andreev-bound *surface* states, which could dominate over and prevent direct tunneling into the *bulk* states. For a model {110} tunnel junction oriented normal to the nodal axis, these surface states are nearly degenerate at the Fermi level, giving rise to a zero-bias conductance peak (ZBCP) which is ubiquitously seen in the cuprates [6,17].

Detailed d-wave tunneling simulations have demonstrated a systematic spectral dependence on both junction *orientation* and *impedance* [13,14]. Specifically, the ZBCP is shown to diminish for either large junction misorientation from the nodal axes or high junction transmission, as the surface states become less robust. Both the antinodal {100} and the c-axis {001} junction models in the low-transmission limit show the expected gap characteristics for quasiparticle tunneling into the bulk d-wave DOS. In the high-transmission limit all junction orientations show the "inverted-gap" characteristics for Andreev reflection based on the same d-wave DOS. These theoretical results suggest that despite the d-wave induced surface states, the bulk DOS may be probed by either reducing the junction impedance or orienting the junction normal to an $\{n0m\}$ axis (n or m = integer) [13,14]. A detailed spectral analysis could then be made to assess the purity of the d-wave order parameter, in particular the amount of s-wave component present.

This Letter addresses these issues *quantitatively* by studying directional tunneling and point-contact spectroscopy on the {100}, {110}, and {001} faces of YBCO single crystals. The conductance spectra show fully developed quasiparticle tunneling, Andreev reflection, and ZBCP characteristics, depending on the junction orientation and impedance. Quantitative spectral analysis using the generalized BTK formalism indicates a predominantly $d_{x^2-y^2}$ pairing symmetry, with less than 5% s-wave component in either the $d + s$ or $d + is$ scenario.

 0031-9007/98/81(12)/2542(4)$15.00

YBCO crystals used for the experiment were grown by a crystal-pulling technique followed by a two-week oxygen annealing [18]. The crystals showed $T_c \approx 90$ K, with ~ 1 K transition, by both resistivity and magnetic susceptibility measurements, and single crystallinity with twinning was verified by x-ray diffraction. Samples with {100}, {110}, and {001} faces were cut from the crystals, using polarized optical microscopy for alignment. The cut crystal faces were polished to optical smoothness, then reannealed in ultrapure O_2 gas at 450 °C for 24 hours followed by slow cooling. The post-annealed samples were subject to controlled chemical etching with 1% Br in absolute ethanol for 1 minute, then ethanol rinsed and dried in ultrapure helium gas, before being loaded for tunneling measurement without exposure to air.

Tunneling and point-contact spectroscopy was performed with a cryogenic scanning tunneling microscope (STM) at 4.2 K in 1 μTorr ultrapure helium, using a piezo-driven Pt-Ir tip. Details of the STM apparatus and tunneling spectroscopy technique are described elsewhere [19]. The point-contact spectra were taken by disabling the STM feedback and pushing the tip into the crystal surface. The STM tunnel junctions were ~ 10 MΩ, and the point-contact junctions were ~ 100 Ω. The latter is larger than the typical impedance for point-contact spectroscopy [20], but well in the Knudsen regime (contact radius $<$ mean free path of YBCO) to assure ballistic transmission with negligible local heating [21].

The current vs voltage I-V data were numerically differentiated into conductance dI/dV and normalized with respect to the spectral background. The representative dI/dV spectra are plotted as open circles in Figs. 1–3, with the sample biased positive relative to the tip. These spectra were reproducible over large areas ($\sim \mu m^2$) on the crystals and over long periods of time ($\sim$hours), with minor variations in the spectral details but no change in the generic spectral features. Figure 1 is for the {110} STM junction, showing a pronounced ZBCP; the left inset is for the {110} point-contact junction, showing a broader peak structure. Figure 2 is for the {100} point-contact junction, showing an inverted-gap hump structure with an asymmetric inflection at zero bias; the left inset is for the {100} STM junction, showing a partially developed U-shaped gap structure with sharp and symmetric gap edges and a ZBCP. Figure 3 is for the {001} STM junction, showing a fully developed V-shaped gap structure with pronounced gap edges which are broadened and asymmetric; {001} point-contact junctions were also measured, but did not show a very different spectral behavior. Similar V-shaped gap structures have previously been seen by STM on $Bi_2Sr_2CaCu_2O_{8+\delta}$ (Bi-2212) [22] and $HgBa_2Ca_{n-1}Cu_nO_{2n+2+\delta}$ (Hg-12($n-1$)n) [19]. Also noteworthy is the kink structure at about double the gap edges in both the {100} and {001} STM data (Figs. 2 and 3), reminiscent of similar features seen by both STM and ARPES on Bi-2212 [11,22] and by STM on Hg-1223 [19].

To explain the variety of spectral behavior observed, we consider a generalized formulation of the BTK theory, which in its original form [16] describes the spectral evolution from quasiparticle tunneling for a dielectric normal/insulator/superconductor $N/I/S$ junction to Andreev reflection for a metallic N/S junction, using a single parameter Z to represent the barrier strength. First, the generalized BTK approach introduced by Hu [13] and Tanaka and Kashiwaya [14] takes explicit account of the phases of the propagating charges, allowing for constructive interference between Andreev-reflected electrons and holes in the junction if they experience phase-reversed pair

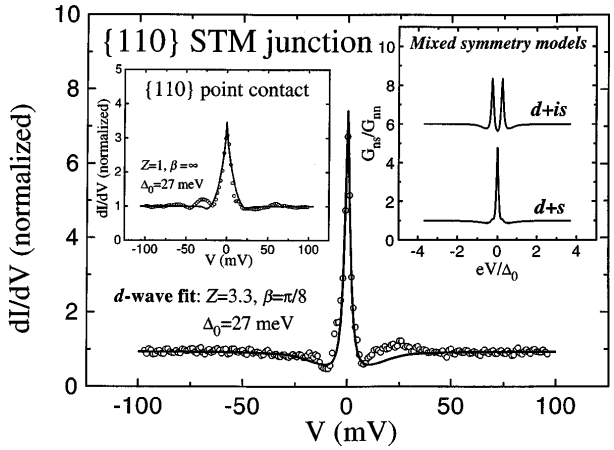

FIG. 1. Normalized conductance spectra taken on the {110} crystal face of YBCO with a Pt-Ir tip at 4.2 K. Main panel is for an STM tunnel junction. Left inset is for a point-contact junction. The data are given as open circles and the d-wave fits by the solid curves. Right inset gives the mixed symmetry simulations for the tunnel junction.

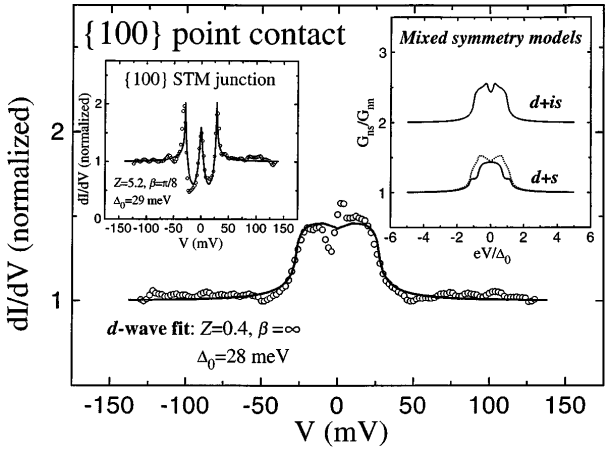

FIG. 2. Normalized conductance spectra taken on the {100} crystal face of YBCO with a Pt-Ir tip at 4.2 K. Main panel is for a point-contact junction. Left inset is for an STM tunnel junction. The data are given as open circles and the d-wave fits by solid curves. Right inset gives the mixed symmetry simulations for the point-contact case (see [30]).

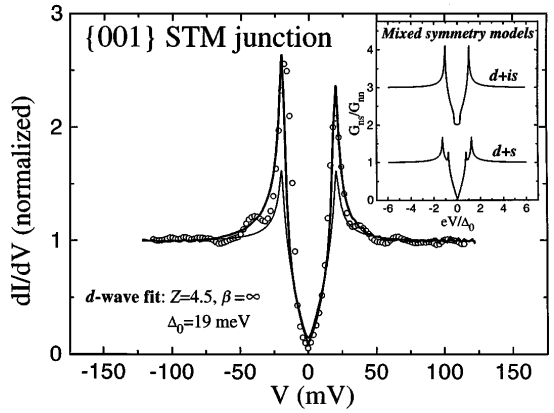

FIG. 3. Normalized conductance data for an STM tunnel junction on the {001} crystal face of YBCO with a Pt-Ir tip at 4.2 K. The data points are shown as open circles. The d-wave fits are given by the thick (band-structure enhanced) and thin (unenhanced) curves. Inset shows the mixed symmetry simulations without the enhancement.

potentials Δ_k. Second, anisotropies in both the Δ_k and the quasiparticle energy E_k can be incorporated by summing the BTK expression over k space [23], with the proviso that the band structure implicit in E_k affect only the normal reflection but not Andreev reflection [24], since the latter entails the formation of Cooper pairs and not quasiparticles. Third, the directionality of transmission can be modeled with a Gaussian "tunneling cone" factor weighting the integration over k_t, i.e., transverse to the junction normal [10,25]. With these modifications the BTK expression for the tunneling current can be written as

$$I_{\mathrm{NS}} = G_{\mathrm{NN}} \int\int e^{-\beta^{-2}k_t^2} d^2k_t \times \int_{-\infty}^{\infty} [1 + A(E_k, \Delta_k, Z) - B(E_k, \Delta_k, Z)] \times [f(E_k - eV) - f(E_k)]\, dE\,, \quad (1)$$

where A and B are the Andreev-reflection and normal-reflection probabilities, f is the Fermi-Dirac function, G_{NN} is the normal-state junction conductance, and β is the tunneling cone width [25]. The generalized BTK kernel $1 + A - B$ is given by [14]

$$\frac{16(1 + |\Gamma_+|^2)\cos^4\theta + 4Z^2(1 - |\Gamma_+\Gamma_-|^2)\cos^2\theta}{|4\cos^2\theta + Z^2[1 - \Gamma_+\Gamma_- \exp(i\varphi_- - i\varphi_+)]|^2}\,, \quad (2)$$

where $\Gamma_\pm = (E/|\Delta_\pm|) - \sqrt{(E/|\Delta_\pm|)^2 - 1}$, and $\exp(i\varphi_\pm) = \Delta_\pm/|\Delta_\pm|$ represents the phase of the pair potential $\Delta_\pm = \Delta(\theta_\pm)$ experienced by an Andreev-reflected electron (or hole) propagating at an angle θ_+ (or $\theta_- = \pi - \theta_+$) relative to the junction normal.

To verify the predominance of d-wave order parameter symmetry in YBCO, the gap function $\Delta_k = \Delta_0(\cos k_x' - \cos k_y')/2 \approx \Delta_0 \cos(2\theta')$ is used in Eq. (1) for spectral analysis, where θ' is defined relative to the a axis. The quasi-two-dimensional (quasi-2D) band structure of YBCO is modeled by the tight-binding dispersion [26], $\xi_k = -2t(\cos k_x' + \gamma \cos k_y') + 4t'(\cos k_x' \cos k_y') - \mu$, with $t = 185$ meV, $t' = 30$ meV, $\gamma = 1.02$, and $\mu = 0.51$ eV, through the relation $E_k^2 = \xi_k^2 + \Delta_k^2$. The tunneling cone width is approximated by setting $\beta = \pi/8$ and $\beta = \infty$, respectively, for the STM *tunnel* junctions and the *point-contact* junctions [25], except for the {001} STM case which has only transverse final states because of the quasi-2D band structure and thus a flat tunneling cone ($\beta = \infty$) [19].

Spectral fits of the d-wave model to our data are shown as solid curves in the figures. In Fig. 1, the ZBCP for the {110} STM junction is successfully fitted with $Z = 3.3$ and $\Delta_0 = 27$ meV, as a clear signature of the Andreev-bound surface states induced by the d wave; while the broader peak for the point-contact junction (left inset of Fig. 1) is accounted for with the same Δ_0 and a lower impedance $Z = 1$. In Fig. 2, the inverted-gap behavior for the {100} point-contact junction is well reproduced, apart from the asymmetric zero-bias inflection, by using $Z = 0.45$ and $\Delta_0 = 28$ meV in a d-wave averaging ($\beta = \infty$) of ordinary Andreev reflection. And for the {100} STM junction (left inset of Fig. 2), the U-shaped gap structure is demonstrated with $Z = 5.2$ and $\Delta_0 = 29$ meV, as a narrow "slice" ($\beta = \pi/8$) of the d-wave antinode; while the ZBCP can be explained as an effect of microfaceting [7,13,27] which allows the surface states of a nodal {110} junction to contribute ($Z = 1.5, \Delta_0 = 29$ meV in the fit). In Fig. 3, the enhanced peak structure for the {001} STM junction can be interpreted as a spectral convolution of the d-wave quasiparticle DOS, which gives a V-shaped gap broadening, and the quasi-2D normal-state DOS, which has a logarithmic singularity near the Fermi level [19,26]. This spectral enhancement is evident by comparing the fit (thick curve in Fig. 3) which considers the normal-state DOS singularity with the other fit (thin curve in Fig. 3) which neglects the singularity, both using $Z = 4.5$ and $\Delta_0 = 19$ meV. For the former fit, the Fermi level is assumed to lie 10 meV above the DOS singularity to account for the peak-height asymmetry, consistent with a slightly underdoped YBCO. It is important to note that both the spectral enhancement and asymmetry for the {001} STM junction case are natural consequences of the flat tunneling cone ($\beta = \infty$), which allows tunneling into the *transverse* quasiparticle states without any cancellation by the *longitudinal* group velocity [28]. The absence of such band-structure effects for all other junction cases follows directly from either: (1) a narrow tunneling cone, which limits the accessible transverse quasiparticle states [19]; or (2) low junction-impedance, which is dominated by Andreev reflection and therefore altogether insensitive to the quasiparticle DOS [24].

Results of the d-wave fits to our data for YBCO are summarized in Table I. The overall spectral consistency among the different junction orientations and impedances further justifies our use of the generalized BTK formalism.

TABLE I. Summary of d-wave fitting results for YBCO using the generalized BTK theory, with β as the tunnel-cone width, Z the barrier strength, Δ_0 the d-wave gap maximum, and $2\Delta_0/k_BT_c$ the reduced-gap ratio.

Junction	β	Z	Δ_0 (meV)	$2\Delta_0/k_BT_c$
$\{110\}$ STM	$\pi/8$	3.3 ± 0.4	27 ± 4	7.0 ± 1.0
$\{110\}$ point contact	∞	1.0 ± 0.2	27 ± 4	7.0 ± 1.0
$\{100\}$ STM	$\pi/8$	5.2 ± 0.5	29 ± 3	7.5 ± 0.8
$\{100\}$ point contact	∞	0.4 ± 0.1	28 ± 3	7.2 ± 0.8
$\{001\}$ STM	∞	4.5 ± 0.5	19 ± 4	4.9 ± 1.0

The error bars in the Z and Δ_0 values reflect spectral variations as well as fitting uncertainties. The difference in the d-wave gap maximum Δ_0 determined from the *in-plane* data ($\Delta_0 \approx 28 \pm 4$ meV) versus the c-axis ($\Delta_0 \approx 19 \pm 4$ meV) data may suggest the need to consider the coupling between the CuO_2 layers [29]. The corresponding $2\Delta_0/k_BT_c$ ratios are larger than the BCS weak-coupling value of 3.54, though comparable to the values reported for other HTSC cuprates [19].

Finally, we consider the mixed symmetry $d + s$ and $d + is$ scenarios to assess the amount of s wave present in YBCO. The gap functions $\Delta_k = \Delta_0 \cos(2\theta') + \Delta_1$ and $\Delta_k = \Delta_0 \cos(2\theta') + i\Delta_1$ are used, respectively, in Eq. (1) for spectral simulations. The simulation results are shown as right insets in the figures, using $\Delta_1/\Delta_0 = 0.25$ and the same Z as in each fit for comparison, and neglecting band-structure effects for simplicity. For the $\{110\}$ STM junction in Fig. 1, $d + is$ splits the ZBCP into broken time-reversal symmetry pairs separated by $2\Delta_1$, while $d + s$ has little effect. For the $\{100\}$ point-contact junction in Fig. 2 [30], both $d + is$ and $d + s$ produce additional spectral kinks, none of which were seen in our data or could explain the asymmetric inflection at zero bias. For the $\{001\}$ STM junction in Fig. 3, $d + is$ flattens out the gap bottom while $d + s$ splits the gap edges by $2\Delta_1$, neither feature being apparent in our data. These spectral comparisons allow us to place an upper limit on any s-wave order-parameter component present in YBCO. From the spectral resolution of our measurement (1 meV) and the results of our spectral analysis (Table I), we estimate less than 5% s wave relative to the predominant d wave in either the $d + s$ or $d + is$ scenario.

In summary, we have studied the directional dependence of quasiparticle tunneling and Andreev reflection on YBCO using the generalized BTK formalism with $d_{x^2-y^2}$ pairing symmetry. STM spectroscopy measurements of $N/I/S$ tunnel and N/S point-contact junctions made on the $\{100\}$, $\{001\}$, and $\{110\}$ crystal faces demonstrate a systematic spectral dependence on the junction orientation and impedance. Quantitative spectral analysis verifies the predominance of d-wave pairing symmetry, with less than 5% s-wave component in either the $d + s$ or $d + is$ scenario.

This work was supported by NSF Grant No. DMR-9705171, NASA/OSS, and the Packard Foundation.

[1] J. F. Annett *et al.*, J. Low Temp. Phys. **105**, 473 (1996); D. J. Scalapino Phys. Rep. **250**, 329 (1995).
[2] C. C. Tsuei *et al.*, Phys. Rev. Lett. **73**, 593 (1994).
[3] D. A. Wollman *et al.*, Phys. Rev. Lett. **71**, 2134 (1993).
[4] A. Mathai *et al.*, Phys. Rev. Lett. **74**, 4523 (1995).
[5] A. G. Sun *et al.*, Phys. Rev. Lett. **72**, 2267 (1994).
[6] M. Covington *et al.*, Phys. Rev. Lett. **79**, 277 (1997).
[7] M. Fogelstrom *et al.*, Phys. Rev. Lett. **79**, 281 (1997).
[8] S. R. Bahcall, Phys. Rev. Lett. **76**, 3634 (1996).
[9] K. A. Kouznetsov *et al.*, Phys. Rev. Lett. **79**, 3050 (1997).
[10] E. L. Wolf, *Principles of Electron Tunneling Spectroscopy* (Oxford University Press, United Kingdom, 1985).
[11] H. Ding *et al.*, Phys. Rev. Lett. **74**, 2784 (1995); Z.-X. Shen *et al.*, Phys. Rev. Lett. **70**, 1553 (1993).
[12] J. R. Kirtley, Phys. Rev. B **41**, 10 (1990); M. E. Flatte and J. M. Byers, Phys. Rev. Lett. **80**, 4546 (1998).
[13] C.-R. Hu, Phys. Rev. Lett. **72**, 1526 (1994); J. H. Xu, J. H. Miller, and C. S. Ting, Phys. Rev. B **53**, 3604 (1996).
[14] Y. Tanaka and S. Kashiwaya, Phys. Rev. Lett. **74**, 3451 (1995); S. Kashiwaya *et al.*, Phys. Rev. B **53**, 2667 (1996).
[15] Ch. Bruder, Phys. Rev. B **41**, 4017 (1990); L. J. Buchholtz *et al.*, J. Low Temp. Phys. **101**, 1099 (1995); M. B. Walker *et al.*, Phys. Rev. B **56**, 9015 (1997).
[16] G. E. Blonder *et al.*, Phys. Rev. B **25**, 4515 (1982).
[17] S. Sinha and K.-W. Ng, Phys. Rev. Lett. **80**, 1296 (1998); L. Alff *et al.*, Phys. Rev. B **55**, 14 757 (1997); J. Geerk *et al.*, Z. Phys. B **73**, 329 (1988).
[18] M. Strasik and D. F. Garrigus (unpublished).
[19] J. Y. T. Wei *et al.*, Phys. Rev. B **57**, 3650 (1998).
[20] G. Deutscher and P. Nozieres, Phys. Rev. B **50**, 13 557 (1994); A. G. M. Jansen *et al.*, J. Phys. C **13**, 6073 (1980).
[21] We estimate the point-contact radius to be $a \approx 45$ Å, using the Sharvin formula for the contact resistance $R_0 = 4\rho l/3\pi a^2$, and taking the normal-state resistivity $\rho \approx 50\ \mu\Omega$ cm and the mean free path $l \approx 100$ Å for YBCO.
[22] C. Renner and Ø. Fisher, Phys. Rev. B **51**, 9208 (1995); Y. DeWilde *et al.*, Phys. Rev. Lett. **80**, 153 (1998); J.-X. Liu *et al.*, Phys. Rev. Lett. **67**, 2195 (1991).
[23] Y. DeWilde *et al.*, Phys. Rev. Lett. **72**, 2278 (1994).
[24] H. F. C. Hoevers, Ph.D. thesis, University of Nijmegen, 1992; P. J. M. van Bentum (unpublished).
[25] In the $N/I/S$ tunneling limit, the Gaussian factor is typically sharp [10], with $\beta^2 = \sqrt{2mU}/\hbar d \approx 0.1$ for a barrier of thickness $d \approx 0.5$ nm, height $U \approx 2.5$ eV, and free electron mass m, thus collimating the transmission within a narrow k_t cone ($\beta \approx \pi/8$) from the junction normal. In the N/S point-contact limit, this cone width becomes infinite ($\beta \to \infty$) as the barrier approaches a delta function ($d \to 0$). For the STM geometry it is thus reasonable to expect a *tunnel* junction (high Z) to be highly k selective, and a *point-contact* junction (low Z) to fully sample the transverse states over k_t.
[26] R. S. Markiewicz, J. Phys. Chem. Solids **58**, 1179 (1997).
[27] Y. Tanuma *et al.*, Phys. Rev. B **57**, 7997 (1998).
[28] W. A. Harrison, Phys. Rev. **123**, 85 (1961).
[29] A. Sudbø and S. P. Strong, Phys. Rev. B **51**, 1338 (1995); S. Chakravarty *et al.*, Science **261**, 337 (1995).
[30] Two orientations are possible (dashed and solid curves in inset of Fig. 2) for the $d + s$ spectral simulation because of the inequivalence between $\{100\}$ and $\{010\}$.